Enantioselective Palladium-Catalyzed Hydrosilylation of Styrene: Influence of Electronic and Steric Effects on Enantioselectivity and Catalyst Design via Hybrid QM/MM Molecular Dynamics Simulations

Alessandra Magistrato,*,† Antonio Togni,‡ and Ursula Rothlisberger§

CNR-INFM-Democritos National Simulation Center and International School for Advanced Studies (SISSA/ISAS), via Beirut 2-4, Trieste, Italy, Department of Chemistry and Applied Biosciences, ETH-Hoenggerberg, HCI, CH-8093 Zürich, Switzerland, and Laboratory of Molecular Chemistry and Biology, EPFL, CH-1015 Lausanne, Switzerland

Received April 2, 2005

The factors determining the enantioselectivity of the palladium-catalyzed hydrosilylation of styrene have been rationalized by performing mixed QM/MM Car−Parrinello molecular dynamics simulations with styrene and 4-(dimethylamino)styrene as substrates. Our results demonstrate that the η^3-benzylic intermediate plays a crucial role in the stereoselectivity of the reaction. The relative thermodynamic stabilities ($\Delta E \approx 1-2$ kcal/mol) of the *endo* and *exo* η^3 forms of the benzylic intermediates, precursors of the two enantiomeric products, are inverted as a function of the electron-releasing or -withdrawing nature of the para substituent of the substrate, and this trend holds also for the transition state of the reductive elimination step (the enantioselectivity-determining step). An electronic and structural characterization of the benzylic diasteroisomers shows that steric effects also play an important role in the inversion of the relative thermodynamic stability of the two allylic diasteroisomers. An analysis of the charge distribution of the free benzyl radical and a computational design of the catalyst suggest that the extent of the chiral induction may be moderately affected by the electronic properties of the substrate, but the sense is mainly dominated by steric effects of both the substrate and the ligands. Finally, we provide suggestions that may increase the observed enantiomeric excess (ee) of the reaction.

1. Introduction

The hydrosilylation of olefins is an important synthetic route to silanes. In combination with an oxidative workup, it has become a method for the one-pot conversion of olefins to alcohols. One of the most common and best known catalysts for this reaction is the Speier catalyst (H_2PtCl_6).[1] Even though the discovery of this synthetic pathway dates back to the late 1940s, it was only much later that an enantioselective version of the hydrosilylation reaction using chiral phosphine ligands was realized.[2] However, this first attempt achieved only modest enantioselectivities (up to 50% ee). Since the catalytic asymmetric functionalization of olefins constitutes a powerful strategy for the synthesis of a variety of optically active compounds,[3] many efforts have been made to optimize the catalysts. More recently, catalysts for asymmetric hydrosilylation of olefins have been reported[4] that in the presence of chiral monodentate phosphine ligands such as MOP[4] afford enantioselectivity (up to 95−99% ee). In these synthetic processes the chiral alkylsilane, formed as a product of the catalytic reaction, is directly oxidized to the corresponding alcohol with complete retention of configuration.[5]

Asymmetric hydrosilylation of olefins[6] has been achieved using chiral ferrocenyl ligands,[7] which have been previously applied to a variety of other reactions.[8−10] Dichloro{1-{(*R*)-1-

* To whom correspondence should be addressed> E-mail: alema@sissa.it.
† CNR-INFM-Democritos Center and International School for Advanced Studies (SISSA/ISAS).
‡ ETH-Hoenggerberg.
§ EPFL.

(1) (a) Speier, J. L. *Adv. Organomet. Chem.* **1979**, *17*, 407. (b) Speier, J. L.; Webster, J. A.; Barnes, G. H. *J. Am. Chem. Soc.* **1957**, *79*, 974. (c) Saam, J. C.; Speier, J. L. *J. Am. Chem. Soc.* **1958**, *80*, 4104. (d) Ryan, J. W.; Speier, J. L. *J. Am. Chem. Soc.* **1964**, *86*, 895.

(2) Brunner, H.; Nishiyama, H.; Itoh, K. In *Catalytic Asymmetric Synthesis*; Ojima, I., Ed.; Wiley-VCH: New York, 1993.

(3) For recent reviews see: (a) *Catalytic Asymmetric Synthesis*, 2nd ed.; Ojima, I., Ed.; Wiley-VCH: New York, 2000. (b) *Comprensive Asymmetric Catalysis*; Jocobsen, E. N., Pfaltz, A., Yamamoto, H., Eds.; Springer: Berlin, 1999**;** Vols. 1−3. (c) Noyori, R. *Asymmetric Catalysis in Organic Synthesis*; Wiley: New York, 1994. (d) Dotta, P.; Kumar, P. G. A.; Pregosin, P. S.; Albinati, A.; Rizzato, S. *Organometallics* **2004**, *23*, 4247. (e) Gade, L. H.; Cesar, V.; Bellemin-Laponnaz, S. *Angew. Chem., Int. Ed.* **2004**, *43*, 1014. (f) Lipshutz, B. H.; Noson, K.; Chrisman, W.; Lower, A. *J. Am. Chem. Soc.* **2003**, *125*, 8779.

(4) (a) Ogasawara, M.; Hayashi, T. In *Catalytic Asymmetric Synthesis*, 2nd ed.; Ojima, I., Ed.; Wiley-VCH: New York, 2000; Chapter 8F, p 651. (b) Hayashi, T. In *Organic Synthesis via Organometallics*; Helmchen, G., Dibo, J., Flubacher, D., Wiese, B., Eds.; Vieweg: Braunschweig, Germany, 1997. (c) Uozumi, Y.; Kitayama, K.; Hayashi, T.; Yanagi, K.; Fukuyo, E. *Bull. Chem. Soc. Jpn.* **1995**, *68*, 713. (d) Uozumi, Y.; Hayashi, T. *J. Am. Chem. Soc.* **1991**, *113*, 9887. (e) Oestereich, M.; Rendler, S. *Angew. Chem., Int. Ed.* **2005**, *44*, 1661.

(5) (a) Tamao, K.; Nakajo, E.; Ito, Y. *J. Org. Chem.* **1987**, *52*, 4412. (b) Tamao, K.; Ishida, N.; Tanaka, T.; Kumada, M. *Organometallics* **1983**, *2*, 1694.

(6) (a) Pioda, G.; Togni, A. *Tetrahedron: Asymmetry* **1998**, *9*, 3903. (b) Pioda, G. Catalisi Asimmetrica: Idrosililazione Enantioselettiva e Ciclizzazione via Trimetilenmetano. Ph.D. Thesis ETH No. 13405, Zürich, Switzerland, 1999.

(7) (a) Togni, A. In *Metallocenes*; Togni, A., Haltermann, R. L., Eds.; VCH: Weinheim, Germany, 1998; Vol. 2, p 685. (b) Togni, A. *Chimia* **1996**, *50*, 86. (c) Togni, A.; Bieler, N.; Burckhardt, U.; Köllner, C.; Pioda, G.; Schneider, R.; Schnyder, A. *Pure Appl. Chem.* **1999**, *71*, 1531. (d) Togni, A.; Dorta, R.; Köllner, C.; Pioda, G. *Pure Appl. Chem.* **1998**, *70*, 1477. (e) Tao, B.; Fu, G. C. *Angew. Chem., Int. Ed.* **2002**, *41*, 3892. (f) Jensen, J. F.; la Cour, T.; Pedersen, H. L.; Johannsen, M. *J. Am. Chem. Soc.* **2002**, *124*, 4558. (g) Barbaro, P.; Bianchini, C.; Giambastiani, G.; Togni, A. *Tetrahedron Lett.* **2003**, *44*, 8279.

10.1021/om050246i CCC: $33.50
Publication on Web 02/04/2006

Table 1. Experimental Enantiomeric Excess (ee) and Calculated Dipole Moments (in debye)[a] as a Function of the Para Substituents of the Substrate[6]

para substituent	% ee	dipole moment
CF_3	58.7 (*S*)	4.02
Cl	67.2 (*S*)	2.33
H	63.4 (*S*)	0.79
Me	46.9 (*S*)	0.23
OMe	6.4 (*R*)	−1.52
NMe_2	64 (*R*)	−2.67

[a] The calculated values refer to the free benzylic radical.

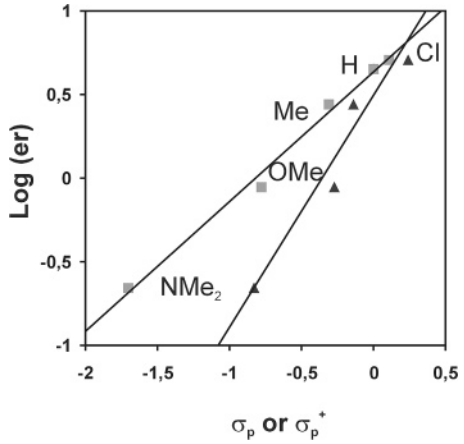

Figure 1. Logarithm of the enantiomeric ratio (log(*S*)/(*R*)) as a function of the Hammett[11] (σ_p, squares) and Brown[12] (σ_p^+, triangles) parameters.

[(*S*)-2(diphenylphosphino-κP)ferrocenyl]ethyl}-3-(2,4,6-trimethylphenyl)-5-1*H*-pyrazole-κN}palladium (**1**) has been successfully utilized for the enantioselective conversion of norbornene,[6] producing *exo*-norborneol in good yields and high enantiomeric excesses up to 99.5%. However, the observed ee is strongly substrate dependent and, using styrenes as substrates, the reaction proceeds with high regioselectivity (99% on the α-carbon), but the ee does not exceed 67%. Interestingly, hydrosilylation reactions, performed on a series of para-substituted styrenes, suggest that the electron-withdrawing or -releasing nature of the para substituent may play a crucial role in determining both the level and the sense of chiral induction. As is apparent from Table 1, the highest selectivity (64% ee) for the *R* form is achieved for 4-(dimethylamino)styrene, whereas the corresponding chloro derivative leads predominantly to the *S* product (67.2% ee). This constitutes a rare example in which a reversal of the enantioselectivity may be induced by the electronic properties of the substrate, as modified by a peripheral substituent.[6] A further indication is given by the quasi-linear dependence of the observed log(er) (er = enantiomeric ratio (*S*)/(*R*)) on the Hammett[11] or Brown[12] parameters (Figure 1).[6b] Since the Hammett and Brown parameters depend uniquely on the electronic properties of the substrate, the observed linear trend suggests an electronic origin for the inversion of ee. Moreover, the fact that the linear correlation fits better with the Brown parameters[12] indicates a build up of a positive charge on the substrate in the enantioselectivity-determining step of the reaction.[6]

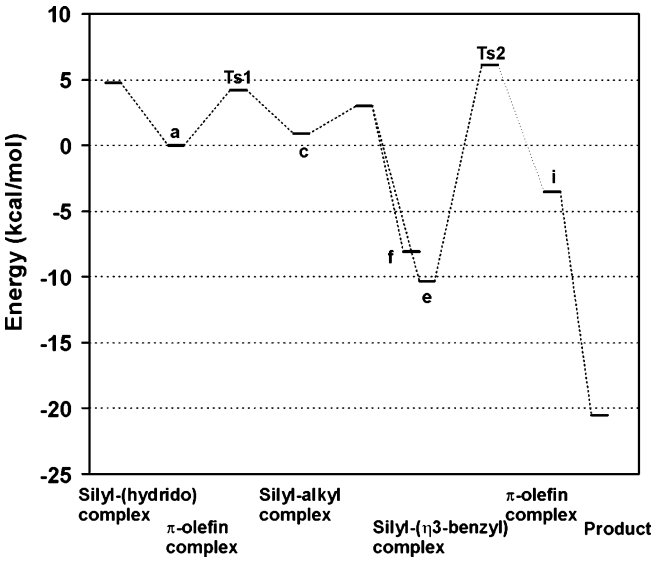

Figure 2. Reaction mechanism for the Pd-catalyzed hydrosilylation of styrene.[13]

The great practical importance of asymmetric hydrosilylation of olefins motivates a characterization of the factors determining the inversion of the enantioselectivity in order to design a catalyst with an improved stereoselectivity.

Recently, we have reported a detailed theoretical investigation of the mechanism of palladium-catalyzed hydrosilylation.[13] The results obtained in our previous study can be summarized in the lowest energy pathway depicted in Figure 2. According to our results,[13] the reaction proceeds in agreement with a classical Chalk−Harrod mechanism,[14] in which the active catalyst for hydrosilylation is a silyl hydrido complex and the coordination of the olefin represents the first step of the catalytic cycle. This is followed by the migratory insertion of styrene into the Pd−H bond with the initial formation of a η^1-alkyl compound. A rearrangement of the substrate converts the η^1-alkyl intermediate into a η^3-benzylic form. The significant energy stabilization due to the formation of the η^3 intermediate offers a rationalization of the observed formation of the Markovnikov regioisomer.[13,15,16] Finally, the reaction proceeds through reductive elimination of the silane and the oxidative addition of a new molecule of trichlorosilane with concomitant regeneration of the active catalyst.[13]

Here, we focused our attention on rationalizing the factors determining the stereoselectivity through mixed quantum/classical (QM/MM) Car−Parrinello[17] molecular dynamic simulations. In QM/MM simulations the chemically relevant part of the system (i.e. the active site of the catalyst) is treated at the quantum mechanical level, while the remaining bulky substituents are treated at the molecular mechanical level.[18] This allows us to treat the chemically relevant part of the system at an accurate level, while still taking into account the steric and electrostatic influence of the remaining part of the system in a

(8) Togni, A.; Burckhardt, U.; Gramlich, V.; Pregosin, P. S.; Salzmann, R.; *J. Am. Chem. Soc.* **1996**, *118*, 1031.
(9) Burckhardt, U.; Baumann, M.; Trabesinger, G.; Gramlich, V.; Togni, A. *Organometallics* **1997**, *16*, 5252.
(10) (a) Schnyder, A.; Togni, A.; Wiesli, U. *Organometallics* **1997**, *16*, 255. (b) Schnyder, A.; Hintermann, L.; Togni, A. *Angew. Chem., Int. Ed. Engl.* **1995**, *34*, 931.
(11) Hansch, C.; Leo, A.; Taft, R. W. *Chem. Rev.* **1991**, *91*, 165.
(12) (a) Okamoto, Y.; Brown, H. C. *J. Am. Chem. Soc.* **1958**, *80*, 4079. (b) Stock L. M.; Brown, H. C. *J. Am. Chem. Soc.* **1959**, *81*, 3323.
(13) Magistrato, A.; Woo, T. K.; Togni, A.; Rothlisberger, U. *Organometallics* **2004**, *23*, 3218.
(14) Chalk, A. J.; Harrod, J. F. *J. Am. Chem. Soc.* **1965**, *87*, 16.
(15) Ludwig, M.; Stroemberg, S.; Svensson, M.; Akermark, B. *Organometallics* **1999**, *18*, 970.
(16) LaPointe, A. M.; Rix, F. C.; Brookhart, M. *J. Am. Chem. Soc.* **1997**, *119*, 906.
(17) Car, R.; Parrinello, M. *Phys. Rev. Lett.* **1985**, *55*, 2471.
(18) Woo. T. K.; Pioda, G.; Rothlisberger, U.; Togni, A. *Organometallics* **2000**, *19*, 2144.

computationally efficient manner.[18] Nowadays, complexes of the size of **1** can be treated entirely at the first-principles level. This serves as a test of the accuracy of the computational scheme adopted, and it provides a reference calculation for the evaluation of different QM/MM models.[18] Once they are validated, these computationally more economical models can also be used to perform efficiently a large number of calculations, and they allow a natural separation of electronic and steric effects.[18]

In view of the small differences in activation (free) energies that are usually involved in the discrimination of two stereoisomers, the characterization of enantioselective reactions and the determination of the factors that govern the stereoselectivity are highly challenging tasks for a computational study. These energy differences are usually close to the limit of accuracy of first-principles calculations. However, since the stereoisomeric complexes that form during the catalytic cycle usually have very similar structures, a fortuitous error cancellation can be highly effective, leading to an unusually high accuracy in predicting relative stabilities. Additionally, the "dynamical simulated annealing" technique, offered by the Car−Parrinello ab initio molecular dynamics (AIMD) scheme, enables an improved search for configurations, which is essential for a reliable investigation of effects within a few kcal/mol. So far, density functional theory (DFT) and hybrid QM/MM methods have been successfully applied to the study of enantioselective reactions,[13,19−21] but never within a mixed Car−Parrinello AIMD QM/MM framework. Therefore, this article represents also a test case study to assess the performance of our computational technique in the treatment of such intricate problems.

2. Computational Section

All of the calculations have been performed with a combined quantum mechanical/molecular mechanics method[22] within the computational scheme of ab initio (Car−Parrinello)[17] molecular dynamics. A number of comprehensive reviews are available on the Car−Parrinello method[23] itself and on applications[24] within a QM/MM framework.

For the part of the system treated at the quantum mechanical level we have performed DFT calculations with the first-principles molecular dynamics package CPMD.[25] This code is based on plane waves, periodic boundary conditions (PBC), and a pseudopotential approach. Gradient-corrected calculations with the exchange functional of Becke[26] and the correlation functional of Perdew[27] have been performed. Moreover, we used an analytical local pseudopotential for hydrogen and norm-conserving nonlocal pseudopotentials of the Martins−Trouiller type[28] for all of the other elements. The valence orbitals have been expanded in a plane wave basis set with a kinetic energy cutoff of 70 Ry. Two models (Figure 3), previously used,[13] have been adopted (see below for a detailed description). All calculations have been performed in periodically repeated face-centered supercells of edge $a = 23$ Å or $a = 24$ Å for QM/MM models B and C, respectively. The geometry optimization runs have been performed with a preconditioned conjugate gradient procedure. For the MD runs, the classical equations of motion were integrated with a velocity Verlet algorithm with a time step of 0.145 fs and a fictitious mass for the electronic degrees of freedom of $\mu = 800$ au. All of the transition states have been determined by performing constrained molecular dynamics runs with increments of 0.1 Å along appropriately chosen reaction coordinates in combination with local optimization techniques. The transition states have been localized by a change of sign of the average constraint force. In addition, we have verified that the localized transition state connects reactants and products by relaxing the geometry of a structure immediately before and after the localized transition state (along the selected reaction coordinate), respectively.

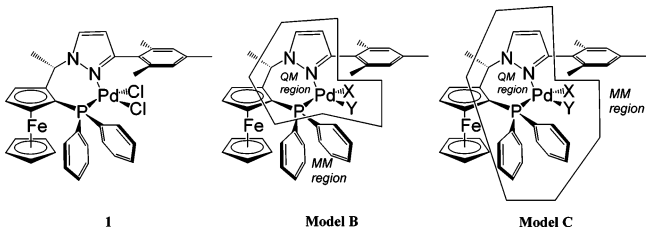

Figure 3. Precursor of the catalyst (**1**) and QM/MM models B and C. The regions included within solid lines represent the quantum mechanical part of the model system.

We have recently developed an interface to the CPMD package in which the coupling with a molecular mechanics force field has been implemented.[29] In this application we have chosen only a mechanical coupling between the QM and the MM subsystems.

For the molecular mechanics potential we have utilized the Tripos 5.2 force field,[30] apart from the ferrocenyl ligand, for which the parameter set of the ferrocene force field of Doman et al.[31] was applied.

Two QM/MM models (Figure 3) have been considered: models B and C. In model B, the mesityl substituent (of the pyrazole) and the phenyls (of the phosphine) have been included in the molecular mechanics part and have been replaced with hydrogen atoms in the QM calculations. Also, the ferrocene is included in the MM part, but it has been replaced with an ethene in the QM region. In addition, to achieve a more realistic model, the double bond of the ferrocene has been constrained to the value found in the crystal structure of **1** (1.465 Å). Model C is an extended version of model B, with the phenyls of the phosphine ligand included in the QM part. This model allows us to test the specific electronic effects of the phenyls on the stereoselectivity of the reaction.

3. Results and Discussion

To rationalize the factors determining the enantioselectivity, we have calculated the relative thermodynamic stabilities of the intermediates of the catalytic cycle, precursors of the two enantiomeric products (model B). In addition, since the *S*-configured product was formed in 63% ee for styrene, whereas

(19) Blöchl, P. E.; Togni, A. *Organometallics* **1996**, *15*, 4125.
(20) (a) Moscardi, G.; Resconi, L.; Cavallo, L. *Organometallics* **2001**, *20*, 1918. (b) Costabile, C.; Cavallo, L. *J. Am. Chem. Soc.* **2004**, *126*, 9592.
(21) (a) Drudis-Sole, G.; Ujaque, G.; Maseras, F.; Llenos, A. *Chem. Eur. J.* **2005**, 11, 1017 (b) Balcells, D.; Maseras, F.; Ujaque, G. *J. Am. Chem. Soc.* **2005**, *127*, 3624.
(22) (a) Singh, U. C.; Kollman, P. A. *J. Comput. Chem.* **1986**, *7*, 718. (b) Field, M. J.; Bash, P. A.; Karplus, M. *J. Comput. Chem.* **1990**, *11*, 700. (c) Review on QM/MM: Gao, J. In *Reviews in Computational Chemistry*; Lipkowitz, K. B., Boyd, D. B., Eds.; VCH: New York, 1996; Vol. 7, p 119.
(23) (a) Remler, D. K.; Madden, P. A. *Mol. Phys.* **1990**, *70*, 691. (b) Payne, M. C.; Teter, M. P.; Allan, D. C.; Arias, T. A.; Joannoppoulos, J. D. *Rev. Mod. Phys.* **1992**, *64*, 1045. (c) Marx, D. Hutter, J. In *Modern Methods and Algorithms of Quantum Chemistry*; Grotendorst, J., Ed.; NIC Series; Forschungzentrum Juelich: Juelich, Germany, 2000; Vol. 1, p 301.
(24) **(24)** (a) Carloni, P.; Rothlisberger, U.; Parrinello, M. *Acc. Chem. Res.* **2002**, *35*, 455. (b) Colombo, M.; Guidoni, L.; Laio, A.; Magistrato, A.; Maurer, P.; Piana, S.; Roehrig, U.; Spiegel, K.; Sulpizi, M.; Vande-Vondele, J.; Zumstain, M.; Rothlisberger, U. *Chimia* **2002**, *56*, 13.
(25) Hutter, J.; Ballone, P.; Bernasconi, M.; Focher, P.; Fois, E.; Goedecker, S.; Parrinello, M.; Tuckerman, M. Max-Planck-Institut für Festkörperforschung and IBM Zurich Research Laboratory, 1995−1996.
(26) Becke, A. D. *Phys. Rev. A* **1998**, *38*, 3098.
(27) Perdew, J. P. *Phys. Rev. B* **1986**, *33*, 8822.
(28) Trouiller, M.; Martins, J. L. *Phys. Rev. B* **1991**, *43*, 1993.
(29) Woo, T. K.; Rothlisberger, U. To be submitted for publication.
(30) Clark, M.; Cramer, R. D., III; Van Opdenbosh, N. *J. Comput. Chem.* **1989**, *10*, 982.
(31) Doman, T. N.; Landis, C. R.; Bosnich, B. *J. Am. Chem. Soc.* **1992**, *114*, 7264.

Table 2. Relative Thermodynamic Stabilities of the *Endo* and *Exo* Isomers Shown in Figure 4 Calculated with Model B[a]

	Δ*E* (kcal/mol)	
isomer	styrene	4-(dimethylamino)styrene
a	0.0	0.0
b	1.6	0.8
c	0.9	0.3
c	5.1	1.6
e	−10.3	−17.2
f	−8.1	−15.6
g	−11.3	−15.5
h	−10.6	−15.3
i	−3.5	
l	−4.2	

[a] All the energies are reported with respect to the *endo* π-olefin complex **a** with styrene and 4-(dimethylamino)styrene as substrates.

4-(dimethylamino)styrene afforded the *R* product with 64% ee,[6] we have performed all calculations with these two substrates. Finally, a quantitative cross-check of the relative energies of selected intermediates has been performed with model C.

3.1. Calculations with Model B.

3.1.1. Hydrosilylation of Styrene. The first step of the catalytic cycle involves the coordination of the substrate to the silyl hydrido form of the active catalyst.[13] Upon formation of the π-complex, the *cis-endo* (**a**) or *cis-exo* (**b**) complexes are the most stable ones among all possible isomers. The *cis* label is due to coordination of the substrate *cis* to the phosphine ligand, while the *endo* or *exo* label is used when the phenyl of styrene is oriented in the same or in the opposite direction of the ferrocene (with respect to the plane defined by the Pd−Si−P atoms), respectively. The *endo* and *exo* isomers are precursors of the two enantiomeric products, by virtue of the coordination of the two enantiofaces of the olefin (R_e for *endo* and S_i for *exo*). The relative energies of the *endo* and *exo* isomers are given in Table 2. The *endo* π-complex is more stable with respect to the corresponding *exo* isomer by −1.6 kcal/mol, and the same trend is observed also for the product of the migratory insertion step, with the *endo* alkyl silyl complex (**c**) being more stable than the *exo* one (**d**) by −4.2 kcal/mol. A rearrangement of the η^1-alkyl ligand leads to η^3 coordination of the benzylic fragment. The formation of such an allylic intermediate occurs in two ways, depending on which one of the two diastereotopic ortho carbons coordinates to palladium. The resulting isomer is termed *syn* or *anti* if the coordinated ortho carbon is *trans* or *cis* with respect to the methyl group,[32] respectively. The *endo* and the *exo syn*/*anti* allylic pairs are depicted in Figure 4e−h.

We have already demonstrated that the significant energy stabilization upon formation of the η^3 intermediate is at the origin of the observed high regioselectivity of >99%.[13] In parallel, an interesting inversion in the relative thermodynamic stabilities of the *endo* and *exo* isomers occurs upon formation of the allylic complexes, with the *exo* form becoming the most stable. In fact, among the four η^3 structures, the *exo-syn* (**g**) and *exo-anti* (**h**) isomers are more stable by −11.3 and −10.6 kcal/mol with respect to the *endo* π-complex. These energies correspond to −10.3 and to −8.1 kcal/mol for the *endo-syn* (**e**) and *endo-anti* (**f**) allylic forms, respectively. Since the *exo* isomers are precursors of the *S* enantiomeric product, their higher thermodynamic stability is in agreement with the enantiomeric *S* excess of 63% observed experimentally (Table 1). A subtle difference of ∼1 kcal/mol is observed in the relative thermodynamic stabilities of the *endo*- and *exo-syn* forms, while this difference increases when considering the *endo*- and *exo*-anti isomers (2.5 kcal/mol). The energy profile of the catalytic cycle is depicted in Figure 5.

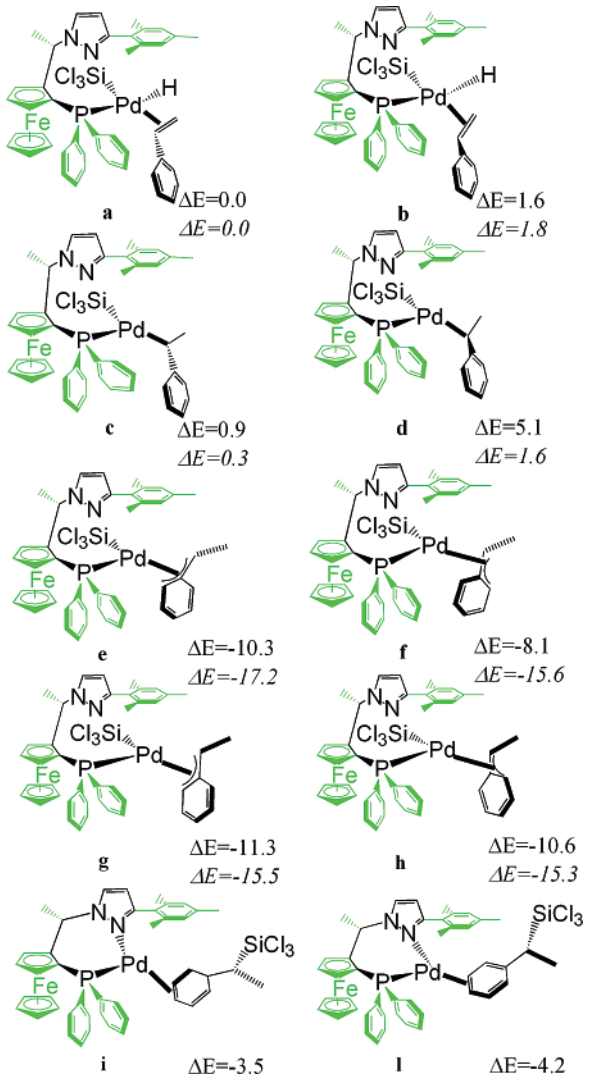

Figure 4. Intermediates of the catalytic cycle with styrene as a substrate (model B). The black and green atoms are included in the QM and MM parts, respectively. **a** and **b** are the *endo* and *exo cis* π-olefin complexes, **c** and **d** are the *endo* and *exo* alkyl silyl complexes, **e**−**h** are the *endo-syn*, *endo-anti*, *exo-syn*, and *exo-anti* η^3 intermediates, and **i** and **l** are reductive elimination products. Relative thermodynamic stabilities (kcal/mol) calculated with respect to **a** are shown. In italics are reported the relative thermodynamic stabilities using 4-(dimethylamino)styrene as a substrate.

The rate-determining step of the catalytic cycle involves the reductive elimination of the silane (TS2).[13] The activation energy barriers, calculated with respect to the corresponding *syn*-allylic forms, are ∼16.4 and ∼16.1 kcal/mol for the *endo* and *exo* isomers, respectively. Thus, the trend in the relative thermodynamic stabilities of the benzylic isomers holds also at the transition state of the reductive elimination step. This attributes a crucial role to the allylic diastereoisomers and their relative thermodynamic stabilities, although the enantioselectivity of the reaction is kinetically controlled by the reductive elimination step.

The transfer of the silyl ligand onto the α-carbon of the substrate is followed by the formation of an intermediate in

(32) The methyl group of the product is formed upon migratory insertion of the styrene in the second step of the catalytic cycle.

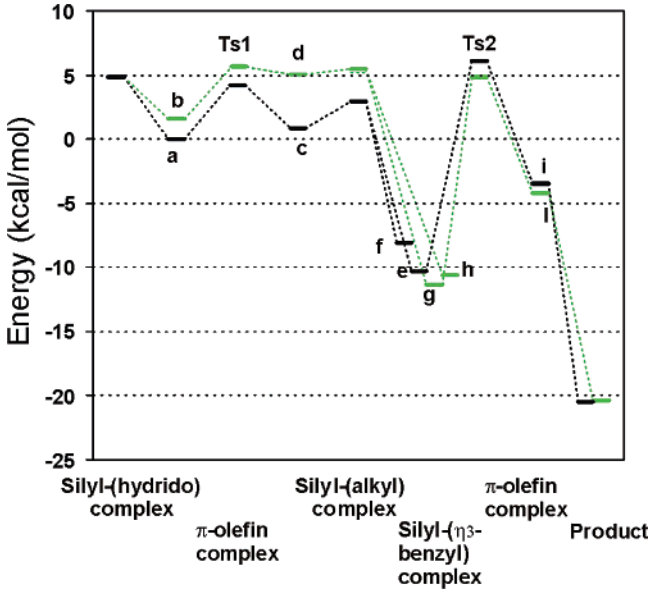

Figure 5. Energy profile of the reaction pathway for the *endo* (black) and *exo* (green) isomers for styrene. Reaction intermediates are labeled as in Figure 4.

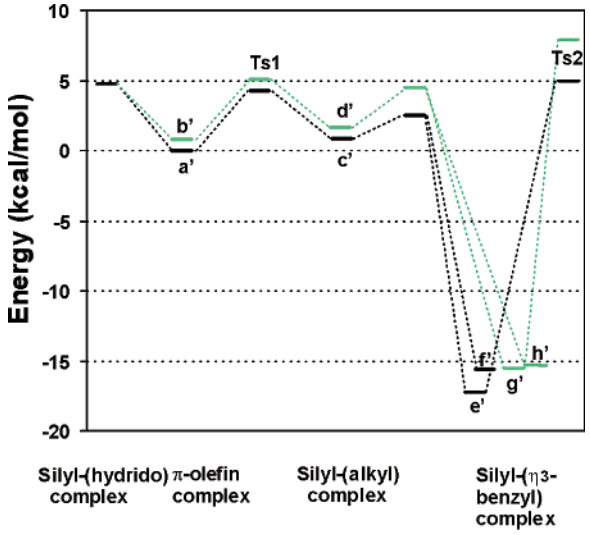

Figure 6. Energy profile of the reaction pathway for the *endo* (black) and *exo* (green) isomers for 4-(dimethylamino)styrene. Reaction intermediates are labeled as in Figure 4.

which the (1-phenylethyl)trichlorosilane product weakly coordinates to palladium (with its phenyl) in an η^2 mode. The corresponding *endo* and *exo* intermediates (**i** and **l**, respectively) are thermodynamically more stable by −3.5 and −4.2 kcal/mol with respect to the *endo* π-complex.

Finally, the oxidative addition of a molecule of trichlorosilane occurs with concomitant liberation of the products. The formation of both *R* and *S* products is exothermic by ∼−20.5 kcal/mol.

3.1.2. Hydrosilylation of *p*-(Dimethylamino)styrene. The calculations performed for styrene show that the enantioselectivity may be correlated with the ΔE of the η^3-benzylic complexes and to the relative activation energies of TS2. However, the observed energy differences are certainly at the limit of accuracy of density-functional calculations. Thus, to verify the accuracy of our results we have recalculated the relative thermodynamic stabilities of *endo* and *exo* isomers for each step of the catalytic cycle using 4-(dimethylamino)styrene (experimentally, this substrate leads to 64% *R* ee).

The *endo* and *exo* isomers considered in our calculations are equivalent to the ones of Figure 4 with the addition of a NMe_2 group at the para position of the substrate.

Using 4-(dimethylamino)styrene, the first part of the reaction pathway is very similar to that computed for styrene. In fact, both the *endo* π and alkyl complexes are thermodynamically more stable than the corresponding *exo* species by −0.8 and −1.3 kcal/mol, respectively. Interestingly, the *endo* isomer is still favored upon formation of the η^3-benzylic intermediates.

The *endo-syn* and *endo-anti* isomers are, in fact, more stable by −17.2 and −15.6 kcal/mol than the *endo*-π-complex, while the *exo-syn* and *exo-anti* forms are more stable by −15.5 and −15.3 kcal/mol, respectively. Thus, the thermodynamically most stable allylic diastereoisomer is here the *endo-syn* derivative (precursor of the *R* product), in agreement with the *R* enantiomeric excess of 64% observed experimentally (with 4-(dimethylamino)styrene). The activation energies of the reductive elimination step are 22.1 and 23.7 kcal/mol for the *endo-syn* and *exo-syn* isomers, respectively. Therefore, the difference in the relative thermodynamic stabilities of the two *endo* and *exo* stereoisomers holds also at the transition state of the reductive elimination step, confirming that the ΔE values of the allylic diastereoisomers may also be correlated with the observed ee values. The energy profile for the reaction pathways of the *endo* and *exo* isomers with 4-(dimethylamino)styrene is reported in Figure 6.

The crucial role played by the allylic form is also in agreement with the observed linear correlation between log(er) and the Brown parameters σ_p^+ (Figure 1).[6] The σ_p^+ parameters have been introduced for reactions involving cationic benzylic species,[12] suggesting the development of a positive charge in the enantioselectivity-determining reaction step (as it occurs in a benzylic species).

To shed light on the origin of the observed ee, we have also inspected the *exo*- and *endo-syn* allylic forms for possible steric discrimination. In this respect, for 4-(dimethylamino)styrene, the *exo-syn* allylic form exhibits a close interatomic contact of 2.47 Å of one hydrogen of the methyl group[32] (Figure 7a) with one hydrogen of one of the *o*-methyl groups of the mesityl substituent, whereas in the *endo-syn* intermediate the closest contact of 2.63 Å concerns the hydrogen of the benzylic carbon (Figure 7b) with the same hydrogen of the mesityl group. The corresponding distances upon η^3 coordination of styrene are 2.51 and 2.53 Å, respectively.

3.2. Calculations with Model C. To validate our findings, we have calculated the relative thermodynamic stabilities of π-olefin and of the *syn* allylic intermediates with model C (Table 3). The structures investigated correspond to complexes **a**, **b**, **e**, and **g** with the phenyls included in the QM part.

This model gives a more realistic description, since it accounts also for the specific electronic contribution of the phenyl substituents. Previous theoretical studies have demonstrated that the electronic properties of phenylphosphines are important factors in determining the structural features of organometallic complexes.[18]

Consistent with the results of model B, in the presence of styrene the *exo*-η^3-benzylic intermediate is more stable than the *endo* form by −1.7 kcal/mol, while the relative stabilities with respect to the *endo* π-complex are −12.9 and −14.6 kcal/mol for the *endo-syn* and *exo-syn* intermediates, respectively. On the other hand, for 4-(dimethylamino)styrene the *endo-syn* complex is more stable than the *exo-syn* species by −2.1 kcal/mol and the relative energies with respect to the *endo*-π

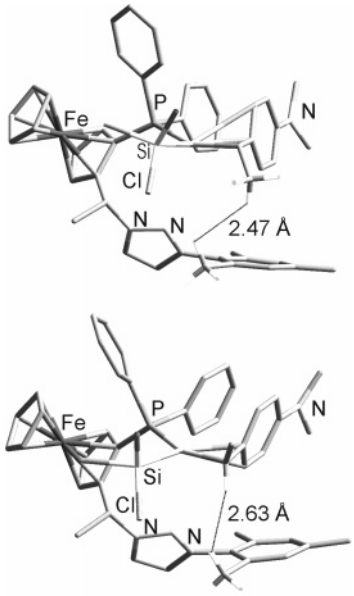

Figure 7. (a) Steric contact between a hydrogen of the methyl group of the substrate and a hydrogen of the mesityl substituent (2.47 Å) for the *exo-syn* intermediate. (b) Steric contact between the hydrogen of the benzylic carbon of the substrate and a hydrogen of the mesityl substituent (2.63 Å) for the *endo-syn* intermediate.

Table 3. Relative Thermodynamic Stabilities of the *Endo* and *Exo* Isomers Calculated with Model C[a]

	ΔE (kcal/mol)	
isomer	styrene	4-(dimethylamino)styrene
a	0.0	0.0
b	4.9	3.5
e	−12.9	−20.4
g	−14.6	−18.3

[a] All of the energies are reported with respect to the *endo* π-olefin complex **a**, with styrene and 4-(dimethylamino)styrene as substrates.

complex are ∼− 20.4 and −18.3 kcal/mol for the *exo-syn* and *endo-syn* forms, respectively. Interestingly, the ΔE values of the *exo-syn* and *endo-syn* forms calculated with the two models are comparable for both styrene (1 and 1.7 kcal/mol for models B and C, respectively, with *exo-syn* being the more stable form) and 4-(dimethylamino)styrene (1.7 and 2.1 kcal/mol, for models B and C, respectively, with *endo-syn* being the more stable form).

In summary, the calculations performed within model C demonstrate an independence of the relative thermodynamic stabilities with respect to the model used.

Additionally, within model C the difference in relative stabilities of the *endo* and *exo*-π-olefin complexes has increased to 4.9 and 3.5 kcal/mol (with the *endo* form being the most stable) for styrene and 4-(dimethylamino)styrene, respectively. The corresponding values using model B were only 1.6 and 0.8 kcal/mol. Thus, the introduction of the phenyl groups in the QM region, as a general feature, enhances the difference in the relative thermodynamic stabilities between the *endo* and the *exo* isomers.

A detailed analysis of possible steric effects has also been performed for the η^3-benzylic intermediates optimized with model C. The measured close steric contacts are 2.54 and 2.49 Å for the *syn-endo* and *syn-exo* allylic forms, respectively, for styrene, while the corresponding values are 2.74 and 2.47 Å for 4-(dimethylamino)styrene. The inclusion of the phenyls in the quantum mechanical region differentiates between the *endo-syn* and *exo-syn* allylic forms in terms of steric effects. In fact, including the phenyls in the QM part, an increase of the distance between parallel phenyl groups (benzylic fragment/phosphine) has been observed. This may be attributed to the presence of $\pi-\pi$ stacking interactions between the two aromatic rings[33,34] that are treated at different levels of theory in models B (fully at the MM level) and C (fully at the QM level), determining a change in the arrangement of the substrate.[33,34]

3.3. Analysis of the Charge Distribution. Searching for simple descriptors for the inversion in the relative thermodynamic stabilities of the η^3 intermediates as a function of the substrate, we have performed an analysis of the charge distribution for the *endo-syn* and *exo-syn* allylic forms (using both styrene and 4-(dimethylamino)styrene). Unfortunately, this search did not show any clear correlation in the charge distribution of the allylic systems (see the Supporting Information), suggesting that electronic effects may not play a major role in the enantioselectivity of the catalytic process.

We have also performed an analysis of the charge distribution[35] on free benzylic radicals as a function of the para substituents, since the linear free energy relationship (Figure 1) suggests that the electronic properties of the substrate itself may affect the enantioselectivity of the hydrosilylation reaction.[6]

This analysis shows a clear correlation between the electron density at the benzylic carbon and the electron-withdrawing or -releasing properties of the para substituent. Indeed, the atomic charge of the benzylic center is −0.21 e with NMe_2 and it decreases monotonically as a function of the electron-withdrawing properties of the substituent, until −0.17 e for CF_3. Since 4-(trifluoromethyl)styrene leads predominantly to the *S* enantiomeric product, the *exo*-allylic form (precursor of the *S* stereoisomer) may be electronically favored by virtue of the delocalization of the electron density toward the aromatic ring of the substrate and a consequent decrease of the electron density on the allylic moiety.

Interestingly, the calculated dipole moments of the free benzylic radicals show an inversion as a function of the para substituent (Table 1).

3.4. Implication for Catalyst Design. In view of our results, we have performed a series of computer experiments (model C) with the aim of providing suggestions that may improve the enantioselectivity of the catalyst.

The first attempt to increase the *S* enantiomeric excess was performed using *p*-cyanostyrene and bis(4-(trichloromethyl)-phenyl)phosphine ligands (D1). By placing electron-withdrawing groups on both the phosphine and the substrate, we should decrease the electron density of the allylic system to a maximum extent.[36]

(33) (a) Magistrato, A.; Merlin, M.; Albinati, A.; Pregosin, P. S.; Rothlisberger, U. *Organometallics* **2000**, *19*, 3591. (b) Magistrato, A.; Pregosin, P. S.; Albinati, A.; Rothlisberger, U. *Organometallics* **2001**, *20*, 4178.

(34) In the case of 4-(dimethylamino)styrene the distance between the nitrogen of the substrate and the para carbon of the phenyl of the phosphine is 3.4 Å in model B, while it increases to 3.6 Å in model C. The observed displacement is probably due to the fact that $\pi-\pi$ stacking interactions, induced by dispersion effects, cannot be described in most DFT methods, as a consequence of the purely local nature of the exchange-correlation approximation (Kristyan, S.; Pulay, P. *Chem. Phys. Lett.* **1994**, *229*, 175). Thus, when both phenyls are included in the QM region (model C), the attractive dispersion interactions between the rings are neglected, leading to a separation of the two rings,[33b] while when one of the two rings in the MM part is included (model B), these interactions between the two aromatic systems are taken into account on a purely empirical basis, via the classical force field approach.[33b]

(35) The calculation of the Mulliken charge distribution of the free benzylic radical was performed using the ADF 2.3 package. The charge analysis has been performed with a double-ζ basis without polarization functions for all atoms.

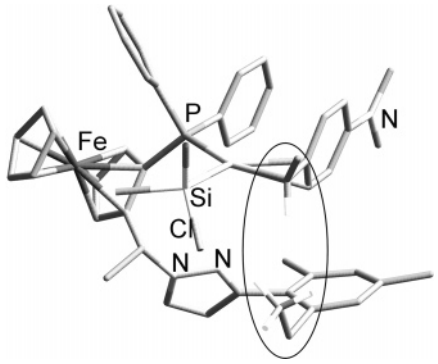

Figure 8. Model system of the *endo-syn* η^3-benzylic intermediate designed to increase the steric contacts between the substrate and the mesityl substituent. One hydrogen of the mesityl substituent has been replaced by a methyl group.

We have analyzed the relative thermodynamic stabilities of the allylic diastereoisomers of D1. The *exo-syn* allylic form is more stable than the *endo-syn* form by −1.3 kcal/mol (ΔE = −1.7 kcal/mol for styrene itself). The decrease in the relative thermodynamic stability of the allylic intermediates with respect to styrene can be attributed to steric contacts between the substrate and the mesityl substituent (2.53 and 2.46 Å (Δd = 0.07 Å) for the *endo* and *exo* allylic forms of D1, versus 2.53 and 2.51 Å (Δd = 0.02 Å) for styrene). Thus, the addition of the para substituents causes closer steric contacts in the *exo-syn* allylic intermediate of D1 with respect to styrene itself. Assuming that ΔE may be directly correlated with the enantioselectivity, this change should not lead to any improvement of the enantioselectivity.

To increase the *R* ee, we placed hydroxyl groups at the para position of the substrate and the phenylphosphine (D2).[36] The presence of electron-releasing groups should increase the electronic density of the allylic system, destabilizing the exo-allylic form on a purely electronic basis. In this case, the exo-syn allylic form of D2 is favored with respect to the *endo* isomer (ΔE = 1.2 kcal/mol). This indicates that also in the presence of an electron-releasing group it is possible to obtain predominantly the *S* enantiomer. The measured steric contacts are 2.52 and 2.46 Å (Δd = 0.06 Å) for the *endo* and *exo* complexes of D2, respectively. Thus, also the hydroxyl groups differentiate between the allylic isomers in terms of steric effects; however, this occurs to a smaller extent as compared to 4-(dimethylamino)styrene (2.63 and 2.47 Å (Δd = 0.16 Å) for the *endo* and *exo* complexes, respectively).

These results, along with other experimental and computational evidences,[37] show that the electronic properties of the substrate may slightly affect the level of the chiral induction, but that the steric hindrance of the substituents induces the most relevant discrimination.

Since it appears impossible to increase the enantiomeric excess by only considering the electronic nature of the para substituents, we have built a new catalyst (model B), increasing its steric hindrance very directionally. To favor the *R* enantiomer, we have replaced the hydrogen of the mesityl group (with which the substrate shows steric contacts) with a methyl group (Figure 8) and we have used 4-(dimethylamino)styrene (D3).[38] As expected, the additional methyl increases the steric contacts between the substrate and the mesityl (the minimal distances are 2.06 and 1.81 Å for the *endo-syn* and the *exo-syn* intermediates of D3, respectively, as opposed to 2.47 and 2.63 Å for the original system).

As a consequence, the *endo-syn* isomer is the most stable and a ΔE value of ∼3.2 kcal/mol is observed between the two *syn*-allylic forms. This greater thermodynamic stability of the *endo-syn* diastereoisomer may increase the ee of the *R* enantiomeric product.

4. Summary and Conclusions

A computational study of the stereoselective Pd-catalyzed hydrosilylation reaction has been performed. On the basis of a previous investigation of the reaction mechanism,[13] we have studied for each step of the catalytic cycle the relative thermodynamic stabilities of the *endo* and *exo* stereoisomers (precursors of the *R* and *S* enantiomeric products, respectively) with different para-substituted styrenes.

An inversion of the relative stabilities of the *endo* and *exo* isomers is observed upon formation of the η^3-benzylic intermediates as a function of the substrate (i.e., the most stable allylic diasteroisomer is always the precursor of the enantiomeric product experimentally in excess); this relative stability holds also at the transition state of the following rate-determining step. This suggests that, although the enantioselectivity is kinetically controlled, the allylic species play a crucial role.

Finally, varying the electronic and steric roles of the para substituents (on both the substrate and the phenylphosphine) and of the mesityl substituent, we have pointed out that the electronic properties of the substrate may slightly affect the level of *S* enantioselectivity, but the sense of the chiral induction is mainly dominated by steric effects.

This theoretical study constitutes a valid contribution in rationalizing the enantioselectivity-determining factors, and finally it provides useful suggestions for a catalyst with improved enantioselective properties.

Supporting Information Available: Tables giving optimized coordinates of equilibrium geometries and transition states and movie files showing the entire catalyst and the reductive elimination step. This material is available free of charge via the Internet at http://pubs.acs.org.

OM050246I

(36) An analysis of the electronic structure shows the presence of an electronic correlation between the allylic system and the diphenylphosphine ligand. See Figure S1 in the Supporting Information.

(37) From the computational point of view, in addition to the presence of strong steric contacts, the importance of steric effects is suggested by the lack of a clear correlation in the charge distribution of the allylic isomers. From the experimental point of view, the observed 67.2% ee using 4-(trifluoromethyl)styrene as substrate does not correlate with the high electron-withdrawing nature of the para substituent (Table 1 and ref 6) and may be caused by the steric hindrance of the para substituent.

(38) Here, the methyl group is used as a simple prototype substituent to increase the steric bulk of the mesityl group very directionally. However, we should point out that isomers with the ethyl rotated by 180° are likely to be thermodynamically favored over the calculated conformer. In addition, we should point out that this is the simplest possible modification that we can do to the catalyst to increase its steric hindrance in a very specific manner. From an experimental point of view it is very unlikely this catalyst could be operative.